ANALYSIS OF INTERNAL TIDE CHARACTERISTICS IN THE NORTHWEST PACIFIC OCEAN

by

Si-Hang XIE[a], Xiao-Jiang ZHANG[a], Xiao-Qun CAO[a,b*], Wen-Long TIAN[b], and Jia-Le YAO[a]

[a] College of Meteorology and Oceanography, National University of Defense Technology, Changsha, China
[b] College of Computer, National University of Defense Technology, Changsha, China

Original scientific paper
https://doi.org/10.2298/TSCI2403335X

The available potential energy of the diurnal internal tide in the Northwest Pacific ocean is studied by using short-term high-frequency mooring observations. The results show that in the upper layer of the ocean, its distribution is relatively chaotic, and it is greater between 1500-1600 m and 2500-3000 m in the middle layer of the ocean. At other depths, it is generally smaller, especially, at the bottom layer of the ocean, it is relatively small. This paper concludes that the marvel of measurement is the best science picks.

Key words: *Northwest Pacific ocean, mooring observations, diurnal internal tide, available potential energy*

Introduction

Fluctuations in the ocean can be categorized according to their location of generation, one category being surface waves, which occur at the surface of the ocean. The other is internal waves, which occur within the densely stabilized stratified ocean. Because the maximum amplitude of internal waves often occurs in the interior of the ocean [1], it is not easy to be directly observed. The wavelengths and periods of internal waves in the ocean are also widely distributed over a wide range, with wavelengths ranging from tens of meters to tens of kilometers, periods ranging from a few minutes to tens of hours, and amplitudes ranging from a few meters to tens of meters. As the most common type of internal waves, internal tides have a very critical role and a unique generation mechanism. Internal tides are a ubiquitous phenomenon of the world ocean, generated when the large-scale barotropic tides flow over varying topographical features in the stratified ocean, such as continental shelf break, sills, or ridges. The generation of internal tides requires the combined action of three elements. Among them, astronomical tides contain powerful energy, which is a necessary condition for the generation of internal tides. The changes of topography will also lead to corresponding changes in the direction of the ocean tidal cycle movement, and the isopycnic inside the ocean will float up and down, and the carrier is seawater which is stably stratified according to density.

As one of the main sinks of astronomical tide energy, internal tides play an important role in maintaining deep-sea mixing and meridional overturning current [2-5]. When

* Corresponding author, e-mail: caoxiaoqun@nudt.edu.cn

the internal tides propagate to the continental slope, as the water depth gradually becomes shallower and the shallowing effects become more and more significant, the movement characteristics of the internal tides change accordingly, resulting in breaking and generating large-scale current and turbulence [6-9]. It has a great impact on maritime transportation, military operations, fishermen operations, and leads to the mixing of nutrients in thermoclines with different densities [10-13]. Internal tides can change the distribution structure of pressure and density by affecting the fluctuation of the isopycnic surface, thereby changing the amplitude, propagation speed and diffusion direction of the acoustic signal in the ocean, and the working effect of sonar will also be greatly affected [14]. The internal tides generated at the source contains multiple vertical modes, among which high-mode internal tides have a shorter wavelength and large vertical shear. Therefore, it is easy for high-mode internal tides to dissipate locally that plays an important role in local mixing [15]. For the low-mode internal tides, because of its longer wavelength and smaller vertical shear, it can propagate to thousands of kilometers away [16], and eventually break up and dissipate in the distant sea, which has a significant effect on the deep mixing [17, 18].

Due to the unique geographical location of the Northwest Pacific ocean and the complex and changeable climate environment, it has created a good platform for people to further study the multi-scale processes of the ocean and its energy evolution [19-22]. In the past scientific research, the large-scale circulation and motion law are the main research directions, and the research on the small and medium-scale processes represented by the internal tides need to be carried out urgently [23-25].

This paper intends to conduct research on the basic characteristics of the internal tides in the Northwest Pacific based on high-frequency mooring observations, to understand the propagation and evolution of the diurnal internal tides in the Northwest Pacific ocean, and to improve our ability to support the environment in the deep sea and sea battlefield. The main research contents include energy distribution characteristics of diurnal internal tides in the Northwest Pacific.

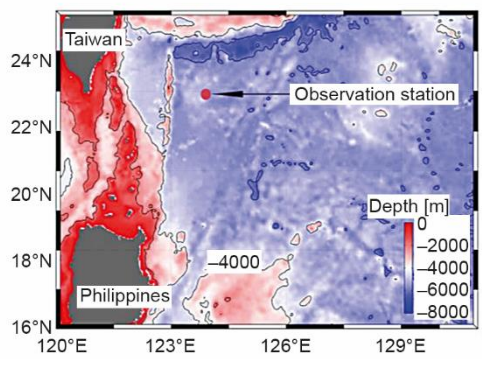

Figure 1. (a) The red dot in the figure is the location of the observation station, and its longitude and latitude are 124°E, 22°N

Data and methods

Mooring observations

The data used in this experiment is the mooring observations obtained by a certain sea-going observation of the College of Meteorology and Oceanography, National University of Defense Technology. The longitude and latitude of the sea area are 124° E, 22° N, as the red dot in the fig. 1 shows. Time and temperature data on 19 different depth layers are obtained with 19 temperature-depth (TD) sensors.

In the subsequent data process, in order to obtain the time and temperature data at other depths, the interpolation method is used to interpolate the existing depth layer data, from 0 m to 5100 m, with an interval of 30 m, so as to obtain the data we need.

Energy

First, using the thermohaline chain and deep-sea CTD observation data, the observed thermohaline profile was vertically interpolated to the 30 m standard layer to obtain the temperature and salinity data and the potential density field data of the whole water depth. According to work done by Desaubies [26], the fluctuations of the isopotential density surface can be calculated by:

$$\tilde{\xi}[\langle z(\sigma_\theta)\rangle_t, t] = \tilde{\xi}(\sigma_\theta, t) = z(\sigma_\theta, t) - \langle z(\sigma_\theta)\rangle_t \tag{1}$$

Next, the vertical flow velocity field can be calculated:

$$\tilde{w}(z,t) = \frac{\partial \tilde{\xi}(z,t)}{\partial t} \tag{2}$$

Referring to the previous work [27-31], the available potential energy (APE) can be integrated over the entire depth using:

$$APE = \frac{1}{2}\rho_0 \int_{-H}^{0} [N^2(z,t)\xi^2(z,t)]_\varphi \mathrm{d}z \tag{3}$$

where H represents the water depth and ρ_0 is the density of seawater. Because the variation in seawater density has little effect on the calculation results of the internal tidal energy, the density of seawater is set as a constant value of 1024 kg/m^3.

Discussion and results

Distribution characteristics of tidal temperature in the Northwest Pacific ocean

We carried out quality control and standard layer interpolation on the acquired mooring observations, deleted some outlier data, and interpolated the data. We set the depth from 0 m to 5100 m, and the interpolation interval was 30 m. From the final result graph fig. 2, it is seen that the temperature decreases gradually from top to bottom, in which the temperature in the upper layer decreases rapidly, and the rate in the lower layer gradually slows down. There is an obvious thermocline in the upper layer.

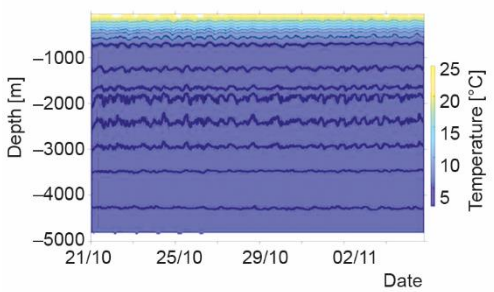

Figure 2. This is the 16-day temperature profiles at the West Pacific ocean fixed point based on the mooring observations, and the horizontal co-ordinates represent the time, ranging from 21 October to 6 November. The vertical co-ordinate represents the water depth, and the color depth represents the temperature magnitude

Available potential energy distribution in the Northwest Pacific ocean

From fig. 3, it can be seen that in the upper layer of the ocean, that is, at a depth of 200-1500 m, from shallow to deep, the distribution of available potential energy of the diurnal internal tide is relatively chaotic. The available potential energy is generally small at the depth between 300 m and 600 m, but it is generally large at the depth between 600 m and 1500 m, and the maximum available potential energy is obtained at the depth between 800 m and 900 m.

From fig. 4, it can be seen that in the middle layer of the ocean, that is, at the depth of 1500-3000 m, from shallow to deep, the available potential energy is generally larger between 1500-1600 m and 2500-3000 m, and generally smaller between 1700-2400 m. The maximum available potential energy is obtained between 1500-1600 m.

From fig. 5, it can be seen that at the bottom layer of the ocean, that is, at a depth of 3000-4500 m, the available potential energy is relatively small in general, only in the depth of 3200-3400 m, the available potential energy is larger, and the maximum value of the available potential energy is also obtained in this depth range.

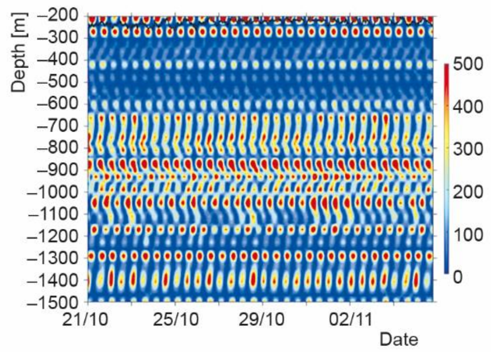

Figure 3. The figure is the available potential energy distribution of diurnal internal tides at the depth of 200-1500 m. Color depth represents the magnitude of the available potential energy

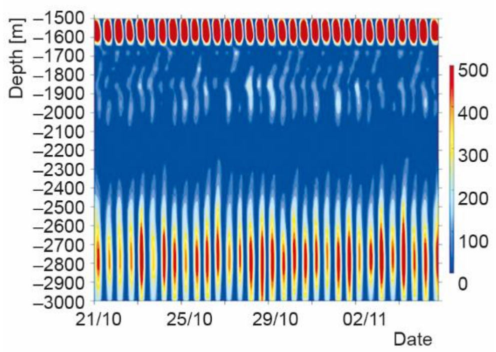

Figure 4. The figure is the available potential energy distribution of diurnal internal tides at the depth of 1500-3000 m. Color depth represents the magnitude of the available potential energy

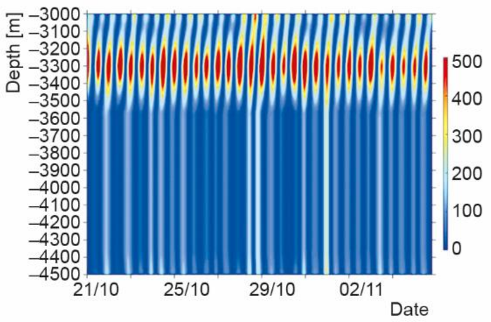

Figure 5. The figure is the available potential energy distribution of diurnal internal tides at the depth of 3000-4500 m. Color depth represents the magnitude of the available potential energy

Conclusion

In this paper, we have analyzed the distribution characteristics of the available potential energy of diurnal internal tides. It is found that the available potential energy is mainly concentrated in the middle and lower layer of the ocean, and it is generally larger in the depth ranging between 1500-1600 m and 2500-3400 m. However, the available potential energy is generally small in the upper layer of the ocean, and the distribution is relatively chaotic, with no obvious distribution law. This paper concludes that the available potential energy of diurnal internal tides in the Northwest Pacific Ocean changes with depth, this finding offers a new window for study the ocean tides.

Acknowledgment

This work is supported by the National Natural Science Foundation of China (Grant No. 41475094) and the National Key R&D Program of China (Grant No. 2018YFC1506704).

References

[1] Garrett, C., *et al.*, Internal tide Generation in the Deep Ocean, *Annu. Rev. Fluid Mech., 39* (2007), Jan., pp. 57-87
[2] Egbert, G. D., *et al.*, Estimates of M2 Tidal Energy Dissipation from TOPEX/Poseidon Altimeter Data, *J. Geophys. Res.: Oceans, 106* (2001), C10, pp. 22475-22502
[3] Munk, W., *et al.*, Abyssal Recipes II: Energetics of Tidal and Wind Mixing, *Deep Sea Res., Part I, 45* (1998), 12, pp. 1977-2010
[4] St. Laurent, L., *et al.*, The Role of Internal Tides in Mixing the Deep Ocean, *J. Phys. Oceanogr., 32* (2002), 10, pp. 2882-2899
[5] Wunsch, C., *et al.*, Vertical Mixing, Energy, and the General Circulation of the Oceans, *Annu. Rev. Fluid Mech., 36* (2004), Jan., pp. 281-314
[6] Holloway, P. E., Internal Hydraulic Jumps and Solitons at a Shelf Break Region on the Australian North West Shelf, *J. Geophys. Res.: Oceans, 92* (1987), C5, pp. 5405-5416
[7] Klymak, J. M., *et al.*, Oceanic Isopycnal Slope Spectra, Part II: Turbulence, *J. Phys. Oceanogr., 37* (2007), 5, pp. 1232-1245
[8] Farmer, D. M., *et al.*, From Luzon Strait to Dongsha Plateau: Stages in the Life of an Internal Wave, *Oceanography, 24* (2011), 4, pp. 64-77
[9] Klymak, J. M., *et al.*, A Simple Parameterization of Turbulent Tidal Mixing Near Supercritical Topography, *J. Phys. Oceanogr., 40* (2010), 9, pp. 2059-2074
[10] Sandstrom, H., *et al.*, Observing Groups of Solitary Internal Waves and Turbulence with BATFISH and Echo-Sounder, *J. Phys. Oceanogr., 19* (1989), 7, pp. 987-997
[11] Sharples, J., *et al.*, Internal Tidal Mixing as a Control on Continental Margin Ecosystems, *Geophys. Res. Lett., 36* (2009), 23
[12] Cacchione, D., *et al.*, Incipient Sediment Movement by Shoaling Internal Gravity Waves, *J. Geophys. Res., 79* (1974), 15, pp. 2237-2242
[13] Johnson, D. R., *et al.*, Internal Tidal Bores and Bottom Nepheloid Layers, *Cont. Shelf Res., 21* (2001), 13-14, pp. 1473-1484
[14] Powell, B. S., *et al.*, Using a Numerical Model to Understand the Connection Between the Ocean and Acoustic Travel-Time Measurements, *The Journal of the Acoustical Society of America, 134* (2013), 4, pp. 3211-3222
[15] Laurent, L. C. S., *et al.*, An Examination of the Radiative and Dissipative Properties of Deep Ocean Internal Tides, *Deep Sea Research Part II: Topical Studies in Oceanography, 51* (2004), 25-26, pp. 3029-3042
[16] Zhao, Z., *et al.*, Global Observations of Open-Ocean Mode-1 M 2 Internal Tides, *J. Phys. Oceanogr., 46* (2016), 6, pp. 1657-1684
[17] Klymak, J. M., *et al.*, The Breaking and Scattering of the Internal Tide on a Continental Slope, *J. Phys. Oceanogr., 41* (2011), 5, pp. 926-945
[18] Zhao, Z., *et al.*, Long-Range Propagation of the Semidiurnal Internal Tide from the Hawaiian Ridge, *J. Phys. Oceanogr., 40* (2010), 4, pp. 713-736
[19] Du, Y., *et al.*, Tropical Indian Ocean Influence on Northwest Pacific Tropical Cyclones in Summer Following Strong El Nino, *J. Clim., 24* (2011), 1, pp. 315-322
[20] Liu, Z., *et al.*, Open Boundary Conditions for Tidally and Subtidally Forced Circulation in a Limited-Area Coastal Model Using the Regional Ocean Modeling System (ROMS), *J. Geophys. Res.: Oceans, 121* (2016), 8, pp. 6184-6203
[21] Hu, D., *et al.*, Pacific Western Boundary Currents and Their Roles in Climate, *Nature, 522* (2015), 7556, pp. 299-308
[22] Chen, C., *et al.*, Role of North Pacific Mixed Layer in the Response of SST Annual Cycle to Global Warming, *J. Clim., 28* (2015), 23, pp. 9451-9458
[23] Xue, H., *et al.*, Kuroshio Intrusion and the Circulation in the South China Sea, *J. Geophys. Res.: Oceans, 109* (2004), C2
[24] Luo, Y., *et al.*, Simulated Response of North Pacific Mode Waters to global warming, *Geophys. Res. Lett., 36* (2009), 23
[25] Liu, Z., *et al.*, Weak Thermocline Mixing in the North Pacific Low-Latitude Western Boundary Current System, *Geophys. Res. Lett., 44* (2017), 20, pp. 10,530-510,539
[26] Desaubies, Y., *et al.*, Reversible and Irreversible Finestructure, *Journal of Physical Oceanography, 11* (1981), 4, pp. 541-556

[27] Alford, M. H., *et al.*, Global Patterns of Low-Mode Internal-Wave Propagation. Part I: *Energy and energy flux, Journal of Physical Oceanography*, *37* (2007), 7, pp. 1829-1848
[28] Huang, X., *et al.*, Role of Mesoscale Eddies in Modulating the Semidiurnal Internal Tide: Observation Results in the Northern South China Sea, *Journal of Physical Oceanography, 48* (2018), 8, pp. 1749-1770
[29] Pickering, A., *et al.*, Structure and Variability of Internal Tides in Luzon Strait, *Journal of Physical Oceanography, 45* (2015), 6, pp. 1574-1594
[30] Waterhouse, A. F., *et al.*, Internal Tide Convergence and Mixing in a Submarine Canyon, *Journal of Physical Oceanography, 47* (2017), 2, pp. 303-322
[31] Zhao, Z., *et al.*, Internal Tides and Mixing in a Submarine Canyon with Time-Varying Stratification, *Journal of Physical Oceanography, 42* (2012), 12, pp. 2121-2142

Paper submitted: December 25, 2022
Paper revised: August 6, 2023
Paper accepted: August 7, 2023